Available online at www.sciencedirect.com

SciVerse ScienceDirect

journal homepage: www.elsevier.com/locate/he

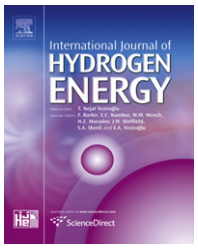

Characteristics of hydrogen-rich gas production of biomass gasification with porous ceramic reforming

Ningbo Gao, Aimin Li, Cui Quan, Yi Qu, Liaoyuan Mao*

School of Environmental Science & Technology, Dalian University of Technology, Key Laboratory of Industrial Ecology and Environmental Engineering, MOE, Dalian, Liaoning 116024, China

ARTICLE INFO

Article history:
Received 10 November 2011
Received in revised form
13 March 2012
Accepted 15 March 2012
Available online 15 April 2012

Keywords:
Biomass
Hydrogen production
Gasification
Kinetics

ABSTRACT

In the present study, an updraft biomass gasifier combined with a porous ceramic reformer was used to carry out the gasification reforming experiments for hydrogen-rich gas production. The effects of reactor temperature, equivalence ratio (ER) and gasifying agents on the gas yields were investigated. The results indicated that the ratio of CO/CO_2 presented a clear increasing trend, and hydrogen yield increased from 33.17 to 44.26 g H_2/kg biomass with the reactor temperature increase, The H_2 concentration of production gas in oxygen gasification (oxygen as gasifying agent) was much higher than that in air gasification (air as gasifying agent). The ER values at maximum gas yield were found at ER = 0.22 in air gasification and at 0.05 in oxygen gasification, respectively. The hydrogen yields in air and oxygen gasification varied in the range of 25.05–29.58 and 25.68–51.29 g H_2/kg biomass, respectively. Isothermal standard reduced time plots (RTPs) were employed to determine the best-fit kinetic model of large weight biomass air gasification isothermal thermogravimetric, and the relevant kinetic parameters corresponding to the air gasification were evaluated by isothermal kinetic analysis.

1. Introduction

As a promising technology for biomass and waste thermochemical conversion, gasification has the advantages of low environmental impact, high effective conversion and reducing global CO_2 emissions [1]. Also, among all biomass conversion technologies, biomass gasification is promising one for hydrogen production. The hydrogen-rich gas production from biomass can be not only directly used in gas turbine for power generation but also catalytically converted into methanol, dimethylether, Fischer–Tropsch oils or other chemical products [2].

During biomass gasification process, the products distribution and the yield of hydrogen-rich synthesis gas depend on the fuel type, reactor configuration, gas–solid residence time, reaction temperature, pressure, gasifying agent and catalyst. Previous works had shown that biomass gasification was performed in various reactors including bubbling fluidized bed reactor [3,4], circulating fluidized bed reactor [1,5], downdraft and updraft fixed bed reactor [6,7] and free-fall reactor [8], etc. To obtain high-grade and clean hydrogen-rich gas, the addition of air, oxygen and/or steam was used as gasifying agent in gasification process. However, one of the most crucial problems of biomass gasification technology is presence of tars and particulates in the produced gas and the hot-gas clean-up, which is the most important challenge to improve the process viability [9]. Extensive studies had carried out on the hot-gas clean-up and tars reforming with catalysts, e.g. calcined

* *Corresponding author*. Tel./fax: +86 411 84707448.
E-mail addresses: nbgao@dlut.edu.cn (N. Gao), leeam@dlut.edu.cn (A. Li).
0360-3199/$ – see front matter Copyright © 2012, Hydrogen Energy Publications, LLC. Published by Elsevier Ltd. All rights reserved.
doi:10.1016/j.ijhydene.2012.03.069

dolomites [10], calcined olivine [11,12], alkali metal [13], Ni-based [9,14] and noble metal [15] catalysts. Although some catalysts do have better effect on hydrogen-rich gas reforming and tar removal, most of them were used as accumulation or layer in reformer and had some problems such as catalyst life, loss activity and carbon deposition. It is found that, under continuous feeding manner, most catalysts often lost their activity due to the sintering of catalyst particles and occurring of carbon deposition, so the practicability of the catalysts employed in gasification reforming might be improved. Porous ceramic might be a promising reforming filling material used in reforming industry. The properties of heat storage capacity, internal surface area and the catalyst came from ceramic composition were utilized to improve producer gas and tars cracking process.

Many researches had investigated the biomass gasification process with common TGA (thermogravimetric analysis) and DTG (derivative thermogravimetry) measurements [16–18]. And sets of formal kinetic parameters for the different biomass types were proposed in the mode of microbalance in which only little weight samples with fine particle materials were investigated. However, the gasification behavior of large weight biomass samples may be closer to the true gasification process. Some researchers had studied the behaviors of biomass isothermal thermo-chemical conversion. Jiao et al. [19] analyzed pyrolysis thermogravity of municipal solid waste used 2 g biomass, and Manyà and Arauzo [20] proposed a kinetic approach to simulate micro-particle pyrolysis of sugar cane bagasse in isothermal conditions. However, lack of research on thermogravimetric analysis of biomass isothermal air gasification with large weight mass (10 g) or more.

Our research team had studied the behaviors of biomass steam gasification with porous ceramic reforming [6]. The producer gas and tars were reformed and converted into small molecule gases after porous ceramic reforming. Although steam gasification is one of the methods for high hydrogen yields, the high heat loss, large energy consuming and the potential contamination condensate produced by excessive steam employed is inevitable. Air and oxygen are most common gasification medium which was widely used in biomass gasification. Unlike steam gasification is endothermic process which demands additional energy cost, air or oxygen gasification process is quite autothermal process. Large amount of experimental studies reported in the literature [7,21–24] showed that the tars produced after condensation in biomass air or oxygen gasification are difficult to further decompose into small molecule gas. Based on the previous study, the process of porous ceramic reforming might be an effective option to tars decomposition and gasification product gas reforming for hydrogen-rich gas production. This paper is the continued study to investigate biomass air and oxygen gasification with porous ceramic reformer for hydrogen-rich gas production. A laboratory scale gasification plant was used to investigate the cracking behavior of large weight biomass. The weight loss of large weight biomass was studied on the laboratory scale thermobalance and the relevant kinetic parameters were determined by an isothermal gasification kinetic model.

2. Experimental

2.1. Biomass sample

The biomass used in this study was pine sawdust which was obtained from a local timber mill (Liaoning province, China). The particle size of this pine feedstock was between 0.2 and 0.4 mm. The low heating value (LHV) and moisture content of the pine sawdust sample were 16.61 MJ/kg and 3.93% on a wet basis, respectively. The ultimate analysis showed that the composition of pine sawdust sample was 44.75% dry and ash-free basis (daf) carbon, 6.31% daf hydrogen, 46.87% (calculated by difference to 100%) daf oxygen, 1.68% daf nitrogen, 0.05% daf sulfur and 0.34% dry basis (db) ash.

2.2. Gasifying process and apparatus

The experiments were performed in a circular in cross-section gasifier, with an inside diameter of 87.5 mm and 1500 mm of total height, a same structure stainless steel cylindrical tube was used as reformer. The detailed presentation of experimental setup was already described in former report [6]. Two identical externally electrical furnaces which provided the heat for gasification and reforming reaction were placed inside gasifier and reformer. A porous ceramic layer was located in the middle of the reformer. Two K-type thermocouples were used to measure the reaction temperature. Feedstock was fed under gravity from the top of the gasifier by a continuous feeding system, which composed of a screw feeder and a variable speed motor. The air and oxygen employed in this study were supplied with an air pump and oxygen cylinder, respectively.

Experimental work was carried out at atmospheric pressure. Hydrogen-rich gas left the gasifier and entered into secondary reformer for tar reforming. After left the reformer, the volume of dry gas, through condensation and drying system, was measured by means of a volumetric gas-meter. Produced gases were collected after 30 min of gasification at steady state. The collected gas-bag was used to collect periodically through a gas syringe and analyzed off-line by gas chromatograph (GC). The gas fraction composition, mainly H_2, CO, CH_4, CO_2 and C_2–C_3 was identified with GC.

2.3. Characterization

The carbon conversion efficiency quantifies the effectiveness of gasification, which is defined in terms of the moles of carbon in the solid biomass that are converted to carbon-containing gases.

Carbon conversion efficiency of biomass, η_c

$$= \frac{12(CO_2 + CO + CH_4 + 2C_xH_y)}{22.4 \times (298/273) \times C(1 - A - M)} G_y \times 100\%,$$

where CO_2, CO, CH_4, C_xH_y (including C_2H_4, C_2H_6, C_3H_6, etc) are gas concentration in vol.%. G_y is producer gas yield. C, A, M are carbon, ash and moisture contents in the ultimate and proximate analysis, respectively.

Low heating value of dry product gas, LHV (kJ/Nm^3)

$$\mathrm{LHV} = 4.18\left(30.0\mathrm{CO} + 25.7\mathrm{H_2} + 85.4\mathrm{CH_4} + 151.3\mathrm{C_xH_y}\right).$$

$$\text{The cold gas efficiency, } \eta_g = \frac{\mathrm{LHV}}{\text{Low heat value of biomass}} G_y \times 100\%$$

In order to investigate the kinetic characteristics of large weight biomass isothermal gasification, a laboratory scale thermobalance was designed, as can be seen from Fig. 1. In this system, the biomass samples were loaded and hung down in the reactor. The heating apparatus worked under certain heating rate, and the electronic balance recorded the sample weight loss simultaneously. To verify the validity of data, all experiments were performed twice. The kinetic parameters were obtained by the isothermal thermogravimetric analysis data, which were acquired using a laboratory scale thermobalance (see Fig. 1). Air as gasifying agent was employed in the case of gasification tests. The continuous measurement of sample weights was performed with an electronic balance to give the instantaneous value of sample residue. The reactor temperatures were controlled in a constant preset level. As the furnace temperature reached the presetting values, certain weight samples (5 g and 10 g) were placed into the hopper and hung down in the reactor. At the same time, the continuous change in the mass of the sample was measured by the electronic balance.

3. Results and discussion

The effects of reactor temperature and equivalence ratio with air and oxygen as gasifying agents on the syngas production were studied.

3.1. *Effect of reactor temperature*

The reactor temperature is one of the most important operating variables for biomass gasification. In this work, the reactor temperatures varied from 1073 to 1223 K in 50 K increments. The equivalence ratio was kept constant at 0.22. Others operating conditions studied in the following range:

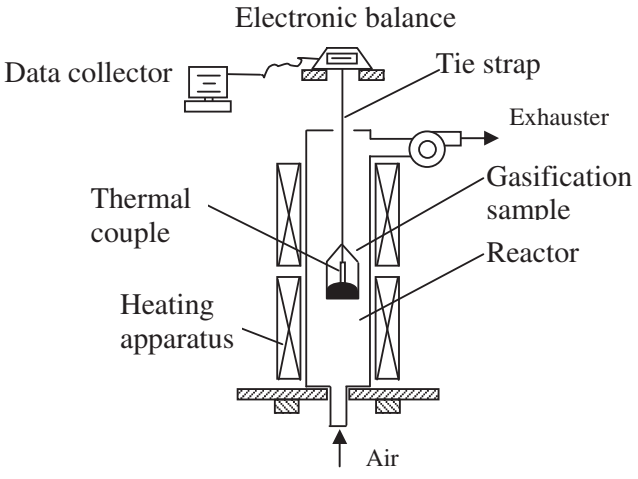

Fig. 1 – A laboratory scale thermobalance scheme.

wet feed rate (kg/h): 0.59, air flowrate: 0.45 l/min, reforming temperature: 1123 K.

The gas composition from different reaction temperatures is shown in Fig. 2(a). It can be clearly seen that H_2 content shows an increasing trend with the rise of the reaction temperature which increases from 21.13 to 27.48% at the reaction temperature range of 1073–1223 K. CO concentration shows an increasing rate as the temperature increased, while CO_2 presents the opposite trend. CH_4 concentration showed a little decrease. These trends can be explained to the following two facts: (1) higher temperatures favored the reactants in endothermic reactions and hinder them in exothermic reactions. (2) The reforming reactions occurred in the porous ceramic zone might enhance hydrocarbon cracking. A simplified gasification mechanism could be explained by using the following reactions [21,25]:

$$\mathrm{Biomass} + \mathrm{O_2} \rightarrow \mathrm{H_2} + \mathrm{CO} + \mathrm{CH_4} + \mathrm{CO_2} + \mathrm{C_xH_y} + \mathrm{Tars} + \cdots,\ \Delta H < 0 \quad (1)$$

$$\mathrm{CH_4} + \mathrm{H_2O} = \mathrm{CO} + 3\mathrm{H_2} + 206\ \mathrm{kJ/mol}; \quad (2)$$

$$\mathrm{C} + \mathrm{H_2O} = \mathrm{CO} + \mathrm{H_2} + 131\ \mathrm{kJ/mol}; \quad (3)$$

$$\mathrm{C} + \mathrm{CO_2} = 2\mathrm{CO} + 172\ \mathrm{kJ/mol}; \quad (4)$$

$$\mathrm{C} + {}^1\!/_2\,\mathrm{O_2} = \mathrm{CO} - 111\ \mathrm{kJ/mol}; \quad (5)$$

$$\mathrm{CO} + \mathrm{H_2O} = \mathrm{CO_2} + \mathrm{H_2} - 41\ \mathrm{kJ/mol}; \quad (6)$$

$$\mathrm{CH_4} + 2\mathrm{H_2O} = \mathrm{CO} + 4\mathrm{H_2} + 165\ \mathrm{kJ/mol}; \quad (7)$$

$$\mathrm{C} + \mathrm{O_2} = \mathrm{CO_2} - 394\ \mathrm{kJ/mol} \quad (8)$$

Without additional water steam fed into the gasifier and reformer, the water content consumed in the above reactions was introduced from the drying zone of the gasifier. According to endothermic reactions (2), (3) and (7), the concentration of H_2 increased with increasing temperature. The endothermic reactions (2)–(4), (7) and exothermic reaction (5) strengthen the concentration of CO. The water–gas shift reaction (6) is reversible and mildly exothermic. At low temperatures the reaction is kinetically limited while at high temperatures it is equilibrium limited. High temperatures favor the reaction moves to the left for CO concentration increase. Guo et al. [24] and Zhou et al. [25] had also found the same trend in biomass air or oxygen gasification. The content of CO was mainly determined by reaction (1) which is an exothermic reaction. Higher temperature was not favorable for CO production, which lead to a CO decrease with temperature increase.

Since porous ceramic was employed for the filler of the reformer, the tars (main include heavy oil vapors, C_1–C_5 hydrocarbons, naphthalin, gas oils and aromatic compounds) produced from biomass gasification process might be trapped by the straight pore embedded in porous ceramic, and in the reforming reaction zone the tars might be decomposed into small molecular gas. The tars might be cracked into a mixture of small mole gases (e.g. H_2, CO, CO_2) under the temperature of 1123 K, and this might contribute to the yields of producer gas. The concentration of C_2–C_3 decreased with the increase of

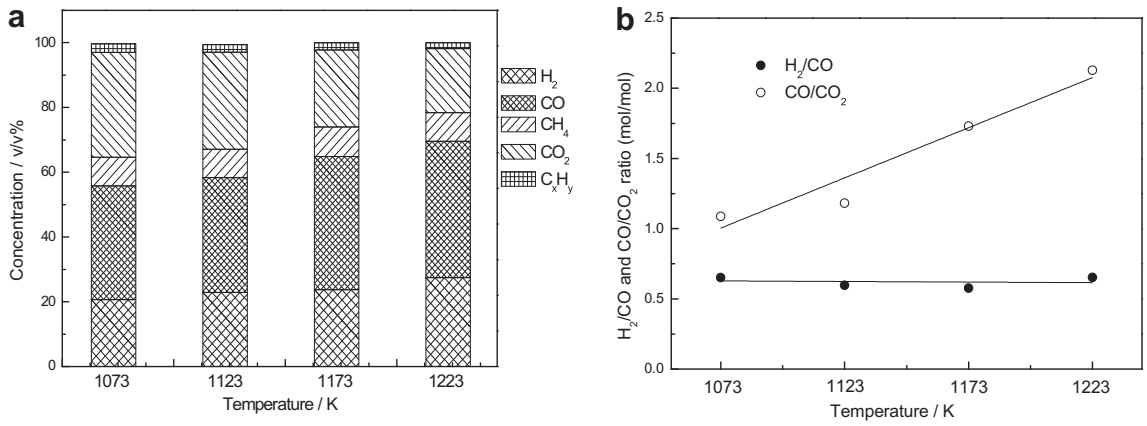

Fig. 2 – Effect of reactor temperature on gas composition (a) and H_2/CO and CO/CO_2 molar ratio (b).

temperature. This reason might be the C_2–C_3 was converted into small molecular gases in the porous ceramic reforming process.

Fig. 2(b) shows the molar ratios of H_2/CO and CO/CO_2 for the product gas at different operation temperatures. In present work, the mole ratio of H_2/CO exhibits a slight fluctuation in the range of 0.58–0.66 mol/mol under the four reaction temperatures. The CO/CO_2 ratio strongly influences the heating value of producer gas. As the ratio increases, the heating value of producer gas grows. With the reactor temperature increasing, the ratio of CO/CO_2 was observed from 1.12 up to 2.12, which presents a clear increase trend. This could be explained that the char reaction with CO_2 and particularly with steam is prevailing [26].

The experimental results were shown in Table 1. Gas yields increased from 1.73 to 2.00 m^3/kg daf biomass in the range of reaction temperature from 1073 to 1223 K, and hydrogen yields rose from 33.17 to 44.26 g H_2/kg biomass. This is due to the fact that the reduced chars and polyatomic hydrocarbons (such as tars) were converted into greater molar quantities of diatomic species such as CO and H_2 [27]. The low heating value (LHV) varied between 6.22 and 7.71 MJ/Nm^3. The changing residence time are not caused by the different air flowrates but exclusively to the different density of the producer gas (lower gas density). Carbon conversion efficiency was found to increase steadily with temperature due to accelerated chemical reaction. Three effect factors could be considered for carbon conversion efficiency in whole temperature range. First, higher temperature strengthened the gasification reactions, and the volatile matters released in gasifier. Second, the cracking and reforming of tars and heavy hydrocarbons trapped on the surface of porous ceramic could occur in the reformer, and finally the adverse effect for carbon conversion is the lower residence time of the gas. These opposite effects exist in gasification and reforming system could be considered for optimizing the operating conditions of a commercial gasification system, as suggested in other works [26]. Cold gas efficiency varied in the range of 60.74–72.63% under different reaction temperatures.

3.2. *Effect of equivalence ratio*

The equivalence ratio (ER) is a crucial factor that affects the performance of the gasification process. ER is defined as the actual oxygen to fuel ratio divided by the stoichiometric oxygen to fuel ratio required for complete combustion. The ER effect on the composition of hydrogen-rich gas produced in air and oxygen gasification was investigated. We had varied ER in the range of 0.18–0.28 and 0.05–0.30 with air and oxygen gasification, respectively. The reactor temperature was kept in 1123 K, wet feed rate was still kept at 0.59 kg/h, air flowrates were varied in the range of 0.36–0.56 for two gasifying agents and the reforming temperature was 1123 K.

The effect of the ER ratio on gas composition in air gasification was shown in Fig. 3(a). It can be seen that H_2 concentration decreased slowly (from 21.69 to 17.26%) and CO

Table 1 – Experimental result of different reactor temperature.

Reactor temperature (K)	Gas yield (m^3/kg daf biomass)	Hydrogen yield (g H_2/kg biomass, dry basis)	Low heating value (MJ/Nm^3)	Residence time (s)	Carbon conversion (%)	Cold gas efficiency (%)
1073	1.73	33.17	6.22	0.34	72.09	60.74
1123	1.77	33.42	6.29	0.36	74.24	63.15
1173	1.9	40.07	7.13	0.34	77.51	71.26
1223	2	44.26	7.71	0.32	75.29	72.63

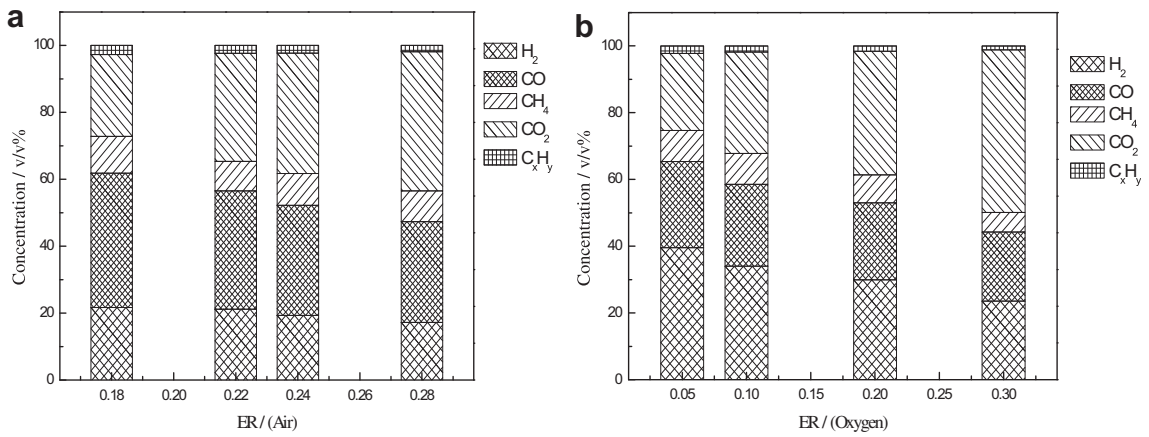

Fig. 3 – Effect of equivalent ratio on gas composition with air (a) oxygen (b) as gasifying agent.

presented a larger decrease (from 40.11 to 30.09%) in the range of ER ratio. CO_2 increased sharply (from 24.40 to 40.57%) with more air was introduced into the reactor. The concentration of CH_4 varied in the range of 8.80–11.03%, C_2–C_3 decreased at low concentration as more air was introduced into gasifier. Fig. 3(b) is the profile of ER ratios effect on gas concentration in oxygen gasification process. The similar trends were observed from Fig. 3(a), the concentrations of H_2 and CO presents a decrease trend from 39.58 to 23.56% and 25.75 to 20.69%, respectively. CO_2 concentration had an apparent increase from 23.13 to 48.74% over the range of increasing ER. CH_4 and C_2–C_3 decreased slowly from 9.36 to 5.83% and 2.20 to 1.18%, respectively. As a comparison of Fig. 3(a) and (b), the similar ER values (0.18 using air and 0.20 using oxygen as gasifying agent, 0.28 using air and 0.3 using oxygen) showed different gas concentration. The reasons of this result might be explained as follows: for air gasification, larger ER values led to more air was introduced into reactor, as a result, large amount of N_2 existed in air was entered into the gasifier. Although N_2 do not take part in the gasification reaction, more heat of reaction zone was carried away with N_2 flow. This leads to the reactor temperature decreasing and the gasification efficiency descending. As ER value increases, more H_2 and CO were oxidized into H_2O and CO_2 (reactions (8) and (10)), and this cause H_2 and CO concentrations decrease and CO_2 concentration increase in the two different gasification modes. On one side, higher ER caused the components of combustible gas loss because oxidize reactions occurred, such as reactions (1), (8) and (9). On the other side, these oxidize reactions could increase the reaction zone temperature, and it strengthens gasification reaction.

$$2CO + O_2 = 2CO_2 - 172.6\ kJ/mol \quad (9)$$

$$2H_2 + O_2 = 2H_2O - 483.6\ kJ/mol \quad (10)$$

The molar ratios of H_2/CO and CO/CO_2 in air and oxygen gasification with varying equivalent ratio were shown in Fig. 4. The molar ratios of H_2/CO of producer gas which value varied between 1 and 2 ($1 < H_2/CO < 2$) could be useful for chemical syntheses, e.g. methanol, pure naphtha production, Fischer–Tropsch (F–T) syntheses (ratio about 2.0) and oxo-synthesis (ratio about 1.0) processes [7,28], etc. The changes of H_2/CO in air gasification increased in the range of ER value from 0.18 to 0.22, and then had a slight decrease trend from 0.22 to 0.28. However, the H_2/CO value of oxygen gasification had a monotonic decrease from 1.13 to 1.5 in the range of ER value from 0.05 to 0.30. Additionally, it is found that the H_2/CO ratio values of these two gasification modes had a large gap (the maximum difference reaches 57% in the same ER value). The results indicated that higher ER values resulted in higher H_2 content consuming in oxygen gasification, while the ratio values showed a low level in the air gasification process. Moreover, compared to air gasification, free nitrogen was introduced into reactor in oxygen gasification, the large amount of heat released and the temperature of reactor rose. As a result, the gasification reaction was improved. The enhanced gasification reactions led to the whole H_2 concentration was far more than that in air gasification. Accordingly, the CO/CO_2 of the two gasification modes shows a quite different trend. An obvious decrease of CO/CO_2 with ER value

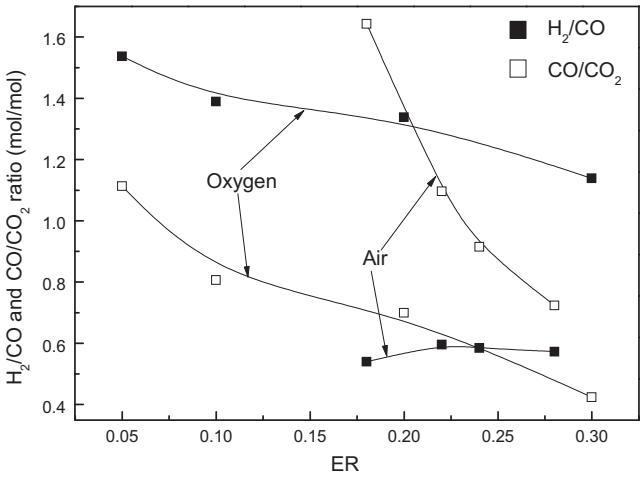

Fig. 4 – H_2/CO and CO/CO_2 molar ratio of air and oxygen as gasification with varying equivalent ratio.

Table 2 – Experimental result of different equivalence ratio with air and oxygen as gasifying agent.

Gasifying agent	ER	Gas yield (m^3/kg daf biomass)	Hydrogen yield (g H_2/kg biomass, dry basis)	Low heating value (MJ/Nm^3)	Residence time (s)	Carbon conversion (%)	Cold gas efficiency (%)
Air	0.18	1.53	29.58	8.18	0.44	64.41	61.43
	0.22	1.77	33.42	6.29	0.36	74.24	63.15
	0.24	1.79	31.5	6.78	0.32	71.04	59.88
	0.28	1.84	29.03	4.48	0.28	86.86	59.56
Oxygen	0.05	1.45	51.29	12.39	6.04	53.01	60.25
	0.1	1.34	38.31	11.22	6.28	58.73	53.96
	0.2	1.24	31.51	10.65	7.02	44.17	39.51
	0.3	1.22	25.68	8.06	6.55	66.06	38.77

increase was observed in air gasification process, while a low level and mild decrease ratio value were presented in oxygen gasification. In Fig. 4, it also can be seen that high CO and low CO_2 concentration were shown in producer gas in the range of ER from 0.18 to 0.28. This might be more CO conversion into CO_2 and more carbon was oxidized into CO_2 in oxygen gasification, which leads to CO_2 concentration higher than CO in the range of ER value from 0.1 to 0.3. While large content N_2 exists in the process of air gasification, higher air flowrate through the reaction zone cause the oxidize reaction incompletely as well as the N_2 taken away plenty of heat in the process of reaction. So, the reaction efficiency of gasification declined.

Table 2 shows the experimental results of different equivalence ratios in air and oxygen gasification. Gas yields increased from 1.53 to 1.84 m^3/kg daf biomass with ER increases from 0.18 to 0.28 in air gasification while the gas yields decreased from 1.45 to 1.22 m^3/kg daf biomass from ER value 0.05–0.3 in oxygen gasification. Under higher ER, more N_2 was introduced into gasifier in air gasification, and the gas yields showed an increasing trend. In oxygen gasification, however, more H_2 was oxidized into H_2O at higher ER values resulted in lower H_2 production. Since the phase transition of steam occurred from gas to liquid in the condensation process, the producer gas yield reduced. As can be seen from Table 2, hydrogen yield reached a maximum value at ER of 0.22 in air gasification, while the maximum H_2 yield was observed at the ER value of 0.05 in oxygen gasification. It can be inferred that the hydrogen yield in the case of pyrolysis (ER = 0) might be higher than that of ER value at 0.05 due to no further oxidized reaction with H_2, CO, CH_4 and other hydrocarbons occurred. The similar trend was observed in other work [25]. However, when the value of ER is equal to zero, the gasification process is entirely endothermic reaction, and it is adverse for the utilization of heat released from biomass itself. Thus, it was not considered in this study. The LHV of producer gas in the two gasification modes showed similar trends which decreased as the equivalence ratio increased. Under different ER values, the residue times of the oxygen gasification were far greater than that of air gasification, which caused the hydrogen-rich gas quality in oxygen gasification is better than that in air gasification. Although the high quality of hydrogen-rich gas was obtained in oxygen gasification, the high price of oxygen comparing with air is an adverse factor for the commercial application. The carbon conversion increased from 64.41 to 86.86% in the range of ER from 0.18 to 0.28 with air gasification, and the similar change was observed in oxygen gasification from 53.01 to 66.06%. Both cold gas efficiency decreased from 61.43 to 59.56% and from 60.25 to 38.77% in the two increase equivalent ratios, respectively.

3.3. *Procedure to determine parameters of reaction kinetics*

3.3.1. *Air gasification reaction isothermal thermogravimetric analysis*

In air gasification, the large weight sample (10 g and 5 g) isothermal TGA curves at four final reaction temperatures (1023, 1073, 1123 and 1173 K) were shown in Fig. 5. According to the experimental results, the great majority of isothermal gasification process was analyzed. The figure shows that the gasification reaction of large weight biomass was characterized by rapid weight losses during the reaction time. At high temperature levels, the gasification reaction presented gradual activity. These curves indicated that adequate temperature is required for high conversion of biomass in a short reaction time condition.

3.3.2. *Parameters of reaction kinetics*

A thermal decomposition and gasification of biomass using air can be given a global reaction as

$$\text{Biomass} + \text{air} \xrightarrow{K} H_2 + CO + CH_4 + CO_2 + C_2 - C_3 + N_2 + \text{Tars} + \text{Char} \quad (11)$$

Kinetic analysis of the isothermal decomposition of biomass is usually based on the following single step kinetic equation:

$$\frac{d\alpha}{dt} = k(T) f(\alpha) \quad (12)$$

where, t is time (s), T is temperature (K), k is rate constant, $f(\alpha)$ is differential form of the kinetic model and is conversion defined as $\alpha = (m_0 - m_t)/(m_0 - m_f)$, m_t is the weight at any time t, and m_0 is the initial weight at the start of that stage, and m_f is the final weight at the end of that stage.

Arrhenius equation expresses the explicit temperature dependency of the rate constant

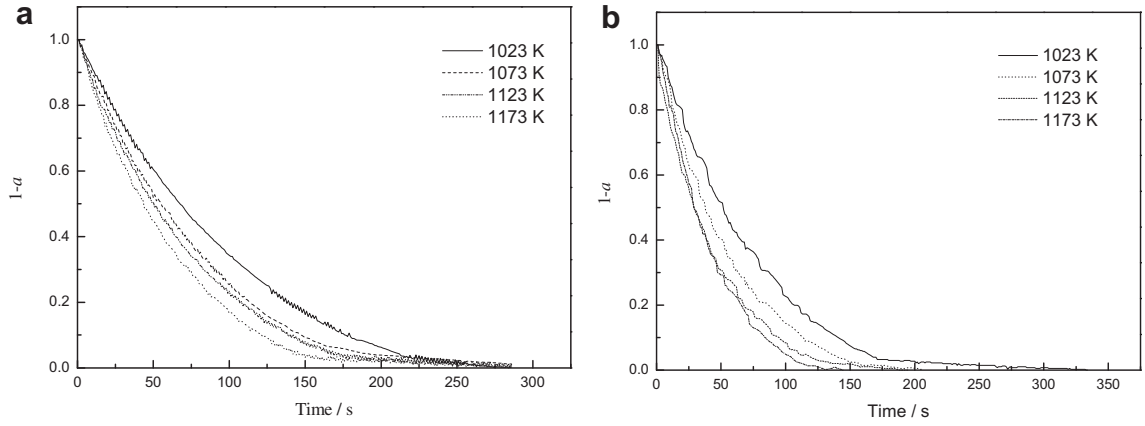

Fig. 5 – Large weight sample of 10 g (a) and 5 g (b) TGA curves of biomass gasification under different final temperatures.

$$\frac{d\alpha}{dt} = Ae^{-E/RT}f(\alpha) \tag{13}$$

where, A is a pre-exponential factor (min^{-1}), E is the activation energy ($J\,mol^{-1}$), R is the universal gas constant (=8.314 $J\,mol^{-1}\,K$). The kinetic model $f(\alpha)$ can be expressed in various forms, as presented in Table 3.

In order to determine the reaction kinetic model, isothermal standard reduced time plots (RTPs) were employed [29]. The experimental and the theoretical RTPs have been constructed by plotting α as a function of a reduced time, t/t_α, where t_α is the time required to obtain a specific conversion. In our study, $\alpha = 0.9$, and $t_{0.9}$, was chosen because in all case final value of α had crossed 0.9. The steps of RTPs obtained are shown as follows [30].

To integrated equation (12), we get

$$g(\alpha) = \int_0^\alpha [f(\alpha)]^{-1}d\alpha = k(T)t \tag{14}$$

If $t_{0.9}$ is the time required to obtain 0.9 fraction reacted, i.e. $\alpha = 0.9$ then

Table 3 – Reaction models employed to describe the biomass gasification reaction [31].

No.	Reaction model	$f(\alpha)$	$g(\alpha)$
1	Power law	$4\alpha^{3/4}$	$\alpha^{1/4}$
2	Power law	$3\alpha^{2/3}$	$\alpha^{1/3}$
3	Power law	$2\alpha^{1/2}$	$\alpha^{1/2}$
4	Power law	$2/3\alpha^{-1/2}$	$\alpha^{3/2}$
5	One-dimensional diffusion	$1/2\alpha^{-1}$	α^2
6	Mample (first-order)	$1-\alpha$	$-\ln(1-\alpha)$
7	Avrami–Erofeev	$4(1-\alpha)[-\ln(1-\alpha)]^{3/4}$	$[-\ln(1-\alpha)]^{1/4}$
8	Avrami–Erofeev	$3(1-\alpha)[-\ln(1-\alpha)]^{2/3}$	$[-\ln(1-\alpha)]^{1/3}$
9	Avrami–Erofeev	$2(1-\alpha)[-\ln(1-\alpha)]^{1/2}$	$[-\ln(1-\alpha)]^{1/2}$
10	Three-dimensional diffusion	$2(1-\alpha)^{2/3}[1-(1-\alpha)^{1/3}]^{-1}$	$[1-(1-\alpha)^{1/3}]^2$
11	Contracting sphere	$3(1-\alpha)^{2/3}$	$1-(1-\alpha)^{1/3}$
12	Contracting cylinder	$2(1-\alpha)^{1/2}$	$1-(1-\alpha)^{1/2}$
13	Second-order	$(1-\alpha)^2$	$(1-\alpha)^{-1}-1$

$$g(\alpha)_{\alpha=0.9} = k(T)t_{0.9} \tag{15}$$

Dividing Eq. (14) by Eq. (15), we obtain the kinetic relationship given as

$$g(\alpha) = (g(\alpha)_{\alpha=0.9})t/t_{0.9} \tag{16}$$

Eq. (16) is dimensionless and is independent of the kinetic rate constant. Thus for a particular reaction mechanism has the unique RTP curve irrespective of the nature of the system, temperature and other factors which affect the reaction rate [30]. Selecting a $g(\alpha)$ which fits the best of the experimental results can be considered as true kinetic model of the studied process. Fig. 6 shows the comparison of experimental RTPs with sample loading of 10 g (a) and 5 g (b) obtained at the temperature of 1023, 1073, 1123 and 1173 K with the RTPs of theoretical kinetic models from Table 3. As can be seen that the reaction kinetic model of contracting sphere (model 11: $f(\alpha) = 3(1-\alpha)^{2/3}$ and $g(\alpha) = 1-(1-\alpha)^{1/3}$) match best with the experimental RTPs.

After identifying the reaction model, $g(\alpha) = 1-(1-\alpha)^{1/3}$ was substituted into Eq. (14), we obtained

$$g(\alpha) = 1-(1-\alpha)^{1/3} = k(T)t \tag{17}$$

And then, we can determine rate constant at a temperature from the slope of a plot of $g(\alpha)$ versus t.

From Eq. (17), the rate constants can be determined at various temperatures, and the E and A that responds to the kinetic model were calculated from Eq. (18).

$$\ln k(T) = \ln A - E/RT \tag{18}$$

So the plot of $\ln k(T)$ against $1/T$ is a straight line with a slope of $-E/R$, and A can be calculated from the Y intercept on the ordinate axis.

According to the experiment data, the Arrhenius plot was shown as Fig. 7(a). The value of activation energy and pre-exponential factor for the gasification reaction stage corresponding to the straight line is obtained from Fig. 7(a). The set of data determined is: $E = 23.797\ kJ\,mol^{-1}$ and $A = 0.0496\ s^{-1}$. Plots of '$\ln k(T)$' against '1000/RT' show good fit ($r^2 > 0.95$) for all samples used in this study.

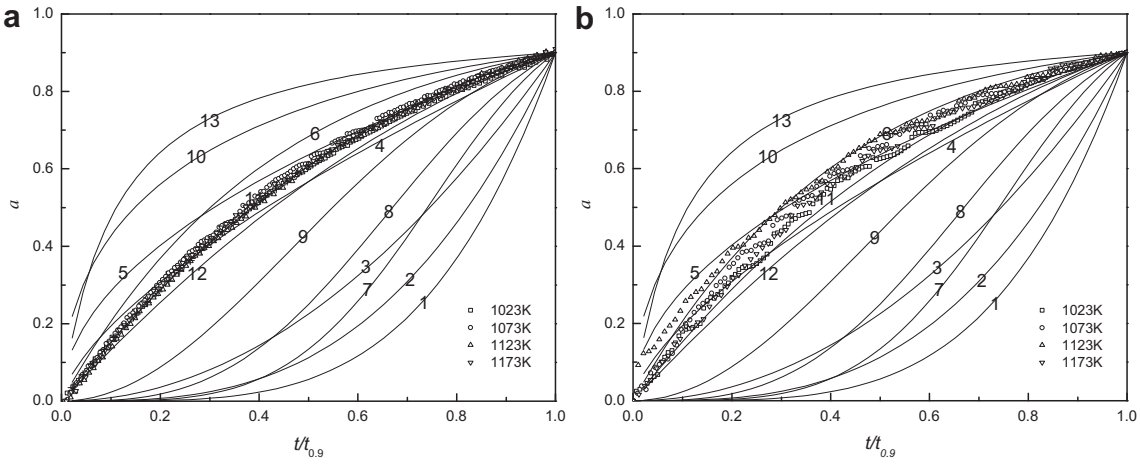

Fig. 6 – Comparison of experimental RTPs with sample loading of 10 g (a) and 5 g (b) at four temperatures of 1023, 1073, 1123, and 1173 K with the theoretic RTPs of the theoretical kinetic models described in Table 3.

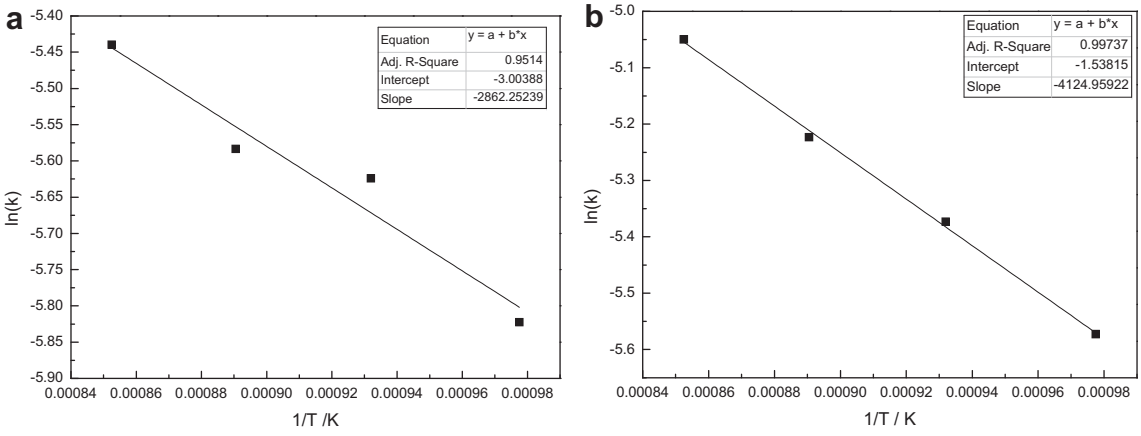

Fig. 7 – Arrhenius plot of biomass gasification with sampling loading of 10 g (a) and 5 g (b) under different final temperatures.

To compare the different weight level for the effect on isothermal weight loss, 5 g weight sample biomass was investigated at four reaction temperatures mentioned above for isothermal TGA (see Fig. 5(b)). Similar with the 10 g weight sample isothermal TGA, higher temperature increase weight loss in the 5 g weight level. And the value of activation energy and pre-exponential factor for the 5 g weight was calculated. The activation energy is 34.295 kJ mol^{-1}, and pre-exponential factor is 0.2148 s^{-1}. It can be seen that two different weight load of samples have different activation energy. It can be concluded that the load of sample has certain effect on activation energy value. In this study, the reason of the difference of activation energy exists might be caused by the reaction heat. Because the reactor has certain heating loss, more heat produced with larger weight sample, and little heat produced with little weight sample. Under the condition of larger reaction heat release, the gasification will be improved, and the activation energy might be lower. However, the less heat was released from the little weight sample loaded cause the relative high heat loss, so the activation energy this might be lower. About the behavior of large weight biomass thermogravity will be investigated in the further study.

4. Conclusions

The hydrogen yields increased from 33.17 to 44.26 g H_2/kg daf biomass in the range of reaction temperature from 1073 to 1223 K. The low heating value (LHV) varied between 6.29 and 7.71 MJ/Nm^3. In air gasification, CO showed a larger decrease in the range of ER ratio while CO_2 increased sharp with the increasing ER value. Hydrogen yields present a maximum value at ER of 0.22 in air gasification, while the maximum H_2 yield is at ER of 0.05 in oxygen gasification. Different weight level sample has different isothermal reaction kinetics. The values of activation energy and pre-exponential factor for the gasification reaction are: $E = 23.797$ kJ mol^{-1} (10 g) and 34.295 kJ mol^{-1} (5 g).

Acknowledgments

The work cited in this paper was supported by the National Natural Science Foundation of China (NSFC) (51006018), China Postdoctoral Science Foundation (No. 20090451264) and by a grant from the National Science and Technology "National water pollution control and management technology major projects" (No. 2008ZX07208-005).

REFERENCES

[1] Li XT, Grace JR, Lim CJ, Watkinson AP, Chen HP, Kim JR. Biomass gasification in a circulating fluidized bed. Biomass and Bioenergy 2004;26:171–93.
[2] Han J, Kim H. The reduction and control technology of tar during biomass gasification/pyrolysis: an overview. Renewable and Sustainable Energy Reviews 2008;12:397–416.
[3] Tzeng LM, Zainal ZA. Operational investigation of a bubbling fluidized bed biomass gasification system. Energy for Sustainable Development 2007;11:88–93.
[4] Lim MT, Alimuddin Z. Bubbling fluidized bed biomass gasification-performance, process findings and energy analysis. Renewable Energy 2008;33:2339–43.
[5] Zhou Z, Ma L, Yin X, Wu C, Huang L, Wang C. Study on biomass circulation and gasification performance in a clapboard-type internal circulating fluidized bed gasifier. Biotechnology Advances 2009;27:612–5.
[6] Gao N, Li A, Quan C, Gao F. Hydrogen-rich gas production from biomass steam gasification in an updraft fixed-bed gasifier combined with a porous ceramic reformer. International Journal of Hydrogen Energy 2008;33:5430–8.
[7] Skoulou V, Zabaniotou A, Stavropoulos G, Sakelaropoulos G. Syngas production from olive tree cuttings and olive kernels in a downdraft fixed-bed gasifier. International Journal of Hydrogen Energy 2008;33:1185–94.
[8] Wei L, Xu S, Zhang L, Liu C, Zhu H, Liu S. Steam gasification of biomass for hydrogen-rich gas in a free-fall reactor. International Journal of Hydrogen Energy 2007;32:24–31.
[9] Świerczyński D, Libs S, Courson C, Kiennemann A. Steam reforming of tar from a biomass gasification process over Ni/olivine catalyst using toluene as a model compound. Applied Catalysis B: Environmental 2007;74:211–22.
[10] Yu QZ, Brage C, Nordgreen T, Sjöström K. Effects of Chinese dolomites on tar cracking in gasification of birch. Fuel 2009; 88:1922–6.
[11] Devi L, Craje M, Thüne P, Ptasinski KJ, Janssen FJJG. Olivine as tar removal catalyst for biomass gasifiers: catalyst characterization. Applied Catalysis A: General 2005;294: 68–79.
[12] Kuhn JN, Zhao Z, Felix LG, Slimane RB, Choi CW, Ozkan US. Olivine catalysts for methane- and tar-steam reforming. Applied Catalysis B: Environmental 2008;81:14–26.
[13] Encinar JM, Beltrán FJ, Ramiro A, González JF. Pyrolysis/gasification of agricultural residues by carbon dioxide in the presence of different additives: influence of variables. Fuel Processing Technology 1998;55:219–33.
[14] Sato K, Fujimoto K. Development of new nickel based catalyst for tar reforming with superior resistance to sulfur poisoning and coking in biomass gasification. Catalysis Communications 2007;8:1697–701.
[15] Nishikawa J, Miyazawa T, Nakamura K, Asadullah M, Kunimori K, Tomishige K. Promoting effect of Pt addition to $Ni/CeO_2/Al_2O_3$ catalyst for steam gasification of biomass. Catalysis Communications 2008;9:195–201.
[16] Yu Z, Ma X, Liu A. Thermogravimetric analysis of rice and wheat straw catalytic combustion in air- and oxygen-enriched atmospheres. Energy Conversion and Management 2009;50:561–6.
[17] Kumar A, Wang L, Dzenis YA, Jones DD, Hanna MA. Thermogravimetric characterization of corn stover as gasification and pyrolysis feedstock. Biomass and Bioenergy 2008;32:460–7.
[18] Li X, Ma B, Xu L, Hu Z, Wang X. Thermogravimetric analysis of the co-combustion of the blends with high ash coal and waste tyres. Thermochimica Acta 2006;441:79–83.
[19] Jiao Z, Yu-qi J, Yong C, Jun-ming W, Xu-guang J, Ming-jiang N. Pyrolysis characteristics of organic components of municipal solid waste at high heating rates. Waste Management 2009; 29:1089–94.
[20] Manyà JJ, Arauzo J. An alternative kinetic approach to describe the isothermal pyrolysis of micro-particles of sugar cane bagasse. Chemical Engineering Journal 2008;139: 549–61.
[21] Cao Y, Wang Y, Riley JT, Pan W-P. A novel biomass air gasification process for producing tar-free higher heating value fuel gas. Fuel Processing Technology 2006;87: 343–53.
[22] Sankar Thanapal S, Annamalai K, Sweeten JM, Gordillo G. Fixed bed gasification of dairy biomass with enriched air mixture. Applied Energy; 2011. doi:10.1016/j.apenergy.2011.11.072.
[23] Gai C, Dong Y. Experimental study on non-woody biomass gasification in a downdraft gasifier. International Journal of Hydrogen Energy 2012;37:4935–44.
[24] Guo X, Xiao B, Liu S, Hu Z, Luo S, He M. An experimental study on air gasification of biomass micron fuel (BMF) in a cyclone gasifier. International Journal of Hydrogen Energy 2009;34:1265–9.
[25] Zhou J, Chen Q, Zhao H, Cao X, Mei Q, Luo Z, et al. Biomass-oxygen gasification in a high-temperature entrained-flow gasifier. Biotechnology Advances 2009;27:606–11.
[26] Franco C, Pinto F, Gulyurtlu I, Cabrita I. The study of reactions influencing the biomass steam gasification process. Fuel 2003;82:835–42.
[27] Wang Y, Kinoshita CM. Experimental analysis of biomass gasification with steam and oxygen. Solar Energy 1992;49: 153–8.
[28] Song X, Guo Z. Technologies for direct production of flexible H_2/CO synthesis gas. Energy Conversion and Management 2006;47:560–9.
[29] Kim S, Kim Y-C. Using isothermal kinetic results to estimate the kinetic triplet of the pyrolysis of high density polyethylene. Journal of Analytical and Applied Pyrolysis 2005;73:117–21.
[30] Bandopadhyay A, Ganguly A, Prasad KK, Sarkar SB, Ray HS. Thermogravimetric studies on the reoxidation of direct reduced iron at high temperature. ISIJ International 1989;29: 753–60.
[31] Erceg M, Kovačić T, Klarić I. Poly(3-hydroxybutyrate) nanocomposites: isothermal degradation and kinetic analysis. Thermochimica Acta 2009;485:26–32.